NASA TECHNICAL NOTE

NASA TN D-4010

NASA TN D-4010
c.1

LOAN COPY:
AFWL
KIRTLAND

TECH LIBRARY KAFB, NM
0130823

LOW-SPEED TESTS OF AN ALL-FLEXIBLE PARAWING FOR LANDING A LIFTING-BODY SPACECRAFT

by Frank M. Bugg and William C. Sleeman, Jr.

Langley Research Center
Langley Station, Hampton, Va.

NATIONAL AERONAUTICS AND SPACE ADMINISTRATION • WASHINGTON, D. C. • JUNE 1967

TECH LIBRARY KAFB, NM
0130823

LOW-SPEED TESTS OF AN ALL-FLEXIBLE PARAWING FOR LANDING A LIFTING-BODY SPACECRAFT

By Frank M. Bugg and William C. Sleeman, Jr.

Langley Research Center
Langley Station, Hampton, Va.

NATIONAL AERONAUTICS AND SPACE ADMINISTRATION

For sale by the Clearinghouse for Federal Scientific and Technical Information
Springfield, Virginia 22151 – CFSTI price $3.00

LOW-SPEED TESTS OF AN ALL-FLEXIBLE PARAWING FOR LANDING A LIFTING-BODY SPACECRAFT

By Frank M. Bugg and William C. Sleeman, Jr.
Langley Research Center

SUMMARY

Low-speed wind-tunnel and flight investigations were made to determine the static longitudinal aerodynamic characteristics and flight-rigging requirements for an all-flexible parawing proposed as a possible landing device for a lifting-body spacecraft.

The maximum lift-drag ratio measured in the wind-tunnel tests of the parawing and lifting-body combination was approximately 2.5 and the maximum lift coefficient obtained was about 0.96. The highest lift-drag ratio measured in this investigation, about 2.7, was obtained with a longitudinal spread of the rigging attachment points at the payload.

Pitching-moment results indicated that the wing-body configuration was stable over the test angle-of-attack range for the assumed moment reference except at the lowest test dynamic pressure, where longitudinal instability occurred at high angles. These results also indicated that for longitudinal control by center-of-gravity shift, a capability of shifting the center of gravity relative to the wing by a distance of 4.2 percent of the body length would allow the parawing-body configuration to be trimmed at any point in its usable lift-coefficient range.

Free-flight tests of the model indicated that the change in length of the three rear lines required to trim the model over its usable lift-coefficient range was about 5 percent of the keel length. In flight tests of the model with a point confluence attachment of the lines, directional alinement characteristics of the body with respect to the wing were unsatisfactory. A modified rigging attachment which provided longitudinal spread of the attachment points at the body was found to give very good directional alinement of the body in flight.

INTRODUCTION

Many research investigations of parawings have been conducted by the National Aeronautics and Space Administration in the past several years. This work has been concerned with several different types of parawing configurations with widely varying geometric, structural, and aerodynamic characteristics. (See refs. 1 to 4.) Most of the

past research has been conducted on parawings having some structural elements such as rigid or inflated-tube leading edges and a spreader bar to fix the wing sweep. Recently the original all-flexible tension-structure parawing concept has been investigated with models of all-fabric lifting surfaces having no structural members or stiffness. These all-flexible parawings are capable of providing gliding, controllable flight through proper rigging of multiple suspension lines which connect the wing to the payload. This type of parawing shows considerable promise for use in applications where compact storage and weight requirements dictate the use of a parachutelike tension structure and where significant glide capability is necessary.

The present investigation was conducted to determine the aerodynamic characteristics and rigging requirements of an all-flexible parawing configuration for possible use as a terminal landing device for a lifting-body spacecraft. The assumption was made that the spacecraft would be configured from considerations of hypersonic aerodynamics with little or no compromise in the body design to provide adequate stability, control, and performance for landing of the body alone. It was also assumed that the subsonic and landing aerodynamic characteristics would be provided by a large all-flexible parawing that could be deployed after reentry in much the same manner as a conventional parachute.

In the present study, static wind-tunnel tests were conducted at low speed to define the longitudinal aerodynamic characteristics for both the parawing and the parawing-body combination with several possible rigging arrangements. In addition, some free-flight tests were made of the wing-body configuration in order to define the rigging geometry for which stable gliding flight can be obtained, and to define the magnitude of pitch control required to trim the model through its usable lift range. Two systems of body attachment points were studied in the flight tests for the purpose of determining possible methods of rigging that would provide good alinement of the body with respect to the wing in flight.

SYMBOLS

The force and moment coefficients are presented with respect to the wind system of axes. The positive directions of forces and moments are shown in figure 1. The moments are given about the reference points shown in figure 2. The reference area used in the reduction of data was the theoretical canopy (flat pattern) area of 43.39 ft^2 (4.031 m^2) and the reference chord was 62.67 in. (1.592 m). The reference chord was taken as the mean aerodynamic chord $\frac{2}{3} l_k$ of the theoretical flat planform. The U.S. Customary System of Units is used with the International System in parentheses.

C_L lift coefficient, Lift/qS

C_D drag coefficient, Drag/qS

C_m	pitching-moment coefficient, Pitching moment/$qS\bar{c}$
L/D	lift-drag ratio
C_T	tension coefficient, Tension/qS
q	dynamic pressure, lb/ft^2 (N/m^2)
S	reference area, ft^2 (m^2)
$\bar{c}$	reference chord, in. (m)
l_k	reference keel length (see fig. 3)
l	line length
x	distance along keel (see fig. 3)
α	angle of attack, deg
α_w	wing angle of attack, measured from vertical to seventh keel line (see fig. 1)

MODEL DESCRIPTION

The parawing was constructed of 1.2 oz/yd^2 (40.5 gm/m^2) acrylic-coated rip-stop nylon. The flat pattern of the wing canopy is shown in figure 3. Loops formed of nylon rope were glued to the wing fabric at the locations shown to make attachment points for the lines. The lines were of 100-lb-test (445-N) nylon cord except for some configurations on which the rear three were of 550-pound-test (2440-N) nylon.

Details of the wind-tunnel model of the spacecraft are shown in figure 2(a) and a photograph of the parawing-body combination in the wind tunnel is given in figure 4. The three rear lines of the wing were attached to eyelets at the corners of the model base and the other lines were clamped between wooden slats in the attachment block. The rigging-spread mount is shown in figure 2(b). The five configurations tested in the wind tunnel are shown in figure 5. These configurations differ in rigging mount, positions of line attachment at rigging mount, and strength of the rear lines, as indicated in figure 5. The line lengths for each configuration are presented in figure 6 and in table I. The lines were measured with a tape measure while hand-held at a tension of approximately

0.5 lb (2.2 N). The relative sizes of the spacecraft and wing were determined by using a full-scale wing loading of 1.0 lb/ft^2 (48 N/m^2) to find the wing size required for a hypothetical spacecraft 35 ft (10.7 m) long and weighing 20 000 lb (88 960 N). The para-wing and spacecraft tested then represented a 0.048-scale model.

The exact differences between the configurations tested in the wind tunnel are not readily apparent in figure 5; however, details of the rigging mounts used are given in figure 2. Configuration A of figure 5 is the wing-body model with a point-confluence rigging except for the three rear lines, which were attached to the rear of the body. A similar rigging arrangement was used for configuration B except that the body was replaced with the rigging-spread mount and the three rear lines were 550-lb test (2440 N) rather than the 100-lb test (445 N) used on configuration A. Configuration C used the same lines as configuration A and the rigging-spread mount; however, the front keel line and the two front leading-edge lines were removed from the confluence and placed in a forward location on the rigging-spread mount. Configuration D was the same as configuration C except that the three rear lines of configuration D were 550-lb test (2440 N). Configuration E was the same as configuration D except that the first two lines of the keel and of each leading edge were placed in a forward location on the rigging-spread mount.

A hollow cast-aluminum spacecraft model wrapped in tape was used with the wing for flight tests. Ballast was added to the model so that its center of gravity was near the midpoint of the body length, as was the moment reference of the wind-tunnel model shown in figure 2(a). The center of gravity of the model-wing combination in flight was not determined because of the difficulty of defining the relative positions of the wing and body in flight and the weight distribution of the lines and wing. The weight of the wing and lines was 0.80 lb (3.6 N) and the weight of the aluminum spacecraft model was 2.75 lb (12.2 N), which gave a wing loading of 0.080 lb/ft^2 (3.83 N/m^2) for the model-wing combination in the flight tests. Details of the two methods of attaching the wing to the spacecraft for flight tests are shown in figure 7. The basic line lengths for the flight tests, which were different from the lengths used in the wind-tunnel tests, are also presented in figure 6 and in table I.

TESTS

Wind-Tunnel Tests and Corrections

Tests were conducted at atmospheric stagnation pressure in the 17-ft (5-m) test section of the Langley 300-MPH 7- by 10-foot tunnel. Static longitudinal aerodynamic characteristics were obtained at 0° sideslip through an angle-of-attack range and through a range of dynamic pressures from 0.50 lb/ft^2 (24 N/m^2) to 1.79 lb/ft^2 (85.8 N/m^2) taken in increments of approximately 0.25 lb/ft^2 (12 N/m^2). At dynamic pressures of

0.50, 1.00, and 1.50 lb/ft^2 (24, 47.9, and 71.8 N/m^2) characteristics were obtained through an angle-of-attack range which was limited for most runs by collapse of the wing nose at low angles and by wing instability at high angles. Before taking data for each configuration, the line lengths were adjusted at a dynamic pressure of 0.50 lb/ft^2 (24 N/m^2) and $\alpha = 0^o$ in an effort to fly the wing at as low a value of α_w as possible. After taking data, these line lengths were measured and they are presented in figure 6 and in table I.

Forces were measured with a sting-supported six-component strain-gage balance. The wing angle α_w was measured visually by means of a protractor mounted on the tunnel window. The sting angle of attack was corrected for structural deflections and jet-boundary effects by using information in references 5 and 6. The wing angle α_w was also corrected for jet-boundary effects. Wake blockage corrections determined from reference 7 were applied to the dynamic pressure.

Flight Tests

The model was dropped from an altitude of approximately 90 ft (27.4 m) by means of a truck-mounted crane and bucket (cherry picker). The altitude lost during deployment was estimated to be less than 30 ft (9.15 m); therefore the altitude remaining for gliding flight was approximately 60 ft (18.3 m). Two methods of attaching the wing to the payload were studied, along with the effect of various rear-line lengths. The wing was hand-held in a folded condition prior to some drops, and for others it was packed in a deployment bag. The flight time was measured with a stop watch. The flights were recorded on film and qualitative comments concerning flight-path angle and payload orientation were recorded.

DISCUSSION

Test Technique

The wind-tunnel tests of the present investigation were different in some important respects from conventional static wind-tunnel tests of rigid aircraft configurations. These differences can impose some difficulties in interpretation of the data, and it is therefore considered appropriate to consider some of the important factors in the testing technique before discussing the test results.

Inasmuch as the wing was completely flexible, the usual methods of mounting the wing on a balance could not be used, and therefore the wing was flown in the tunnel by means of suspension lines attached to a strain-gage balance through the body or rigging mount. For all test conditions at which data were obtained, the wing itself was in steady trimmed flight. The operational range of lift coefficients was generally determined in

the tunnel tests by collapse of the nose at low angles and by a Dutch-roll type of lateral instability at high angles.

The importance of proper setting of the line lengths was recognized in early wind-tunnel tests of all-flexible parawings, particularly when trimming the wing for best L/D. It was found that relatively small changes in line length – as small as $0.002l_k$ – were important, particularly for the three rear lines. The rigging lengths presented herein may therefore be subject to some modification in attempting to reproduce the test results on similar models, particularly if the lines have different elastic properties from those used in the present tests. The same observation can be made with respect to the elastic properties and fabric orientation of the wing canopy.

Wind-Tunnel Tests

Aerodynamic characteristics of wing-body configurations.- The longitudinal aerodynamic characteristics of the wing-body combination (configuration A) over the test angle-of-attack range are presented in figure 8(a) for three values of dynamic pressure. The lift coefficient changed very little with increasing angle of attack for the fixed rigging used. The maximum lift coefficient obtained was about 0.96. The lift-drag ratios generally decreased with increasing angle of attack and were highest for the highest dynamic pressure. The highest lift-drag ratio obtained with the wing-body configuration was about 2.5 and occurred near 0^o angle of attack. A low body angle for maximum lift-drag ratio is important to allow good pilot visibility for landing a manned spacecraft.

The data in figure 8(a) show a large variation in wing angle of attack with body angle of attack and with test dynamic pressure. At the lowest dynamic pressure the change in wing angle was about equal to the change in body angle, whereas at the highest dynamic pressure the wing angle increased about $1/2^o$ for a 1^o increase in body angle. The wing angle at a given body angle of attack decreased with increasing dynamic pressure. A comparison of lift-drag ratios and wing angles shows that the highest lift-drag ratios accompanied the lowest wing angles of attack, and the highest values of lift-drag ratio occurred at the highest test dynamic pressure. It is of interest to note that the dynamic pressures used in the tests were representative of full-scale values for a lift coefficient of 1.0, for which the flight dynamic pressure would be equal to the wing loading.

The increase in lift-drag ratio with increasing dynamic pressure may have been caused by several factors; however, the most important factor was probably favorable aeroelastic effects that accompanied increases in dynamic pressure. The line-tension coefficients presented in figure 9 indicate that wing-tip lines carried about twice as much load as the most highly loaded of the other lines. Computation of the stretch in the rear keel and tip lines indicated that the elongation under load was about $0.0042l_k$ in the keel line and $0.01l_k$ in the tip lines. The greater elongation in the rear lines in comparison

with the other lines caused the wing to trim at a lower angle of attack, and therefore at a higher lift-drag ratio, for the higher dynamic pressures. This favorable effect of elongation of the rear lines, however, does not fully account for the observed increases in lift-drag ratio, inasmuch as similar changes applied to the line lengths at lower dynamic pressure did not improve the lift-drag ratios.

Experience obtained in rigging the wing for best L/D indicated that the lift-drag ratio increased as the rear lines were lengthened until the stagnation point at the nose moved from the lower surface to the upper surface. The movement of the stagnation point caused the nose to collapse back to the second keel line. Curvature observed in the forward lines indicated that the nose was very lightly loaded when the wing was trimmed for maximum lift-drag ratio at a low dynamic pressure. An increase in dynamic pressure would therefore be expected to increase the load on the nose portion in relation to the weight of the lines and canopy, and thereby delay nose collapse to a lower angle of attack.

The parawing used in the present investigation was a flexible, aeroelastic lifting surface, and therefore increased aerodynamic load and changes in line length due to elongation would be expected to cause changes in the canopy shape. Information on canopy shape was not obtained in this investigation, and consequently no assessment can be made of the effects of loading and rigging on canopy shape other than the aforementioned canopy-nose behavior.

The pitching-moment data presented in figure 8(a) indicate that at the highest dynamic pressure the wing-body configuration was stable over the test angle-of-attack range for the assumed moment reference. Results obtained at the lowest dynamic pressure, however, show an instability at the higher angles of attack. This instability at the lowest dynamic pressure is believed to have occurred because of the onset of wing stall and attendant flow separation, as evidenced by the increased drag and slight reduction in lift at the highest angle of attack. This instability could limit the lower range of wing loadings of interest for this configuration. The pitching-moment data of figure 8(a) also indicate that the model was not in trim with respect to the particular moment reference used. The model tested was a hypothetical configuration, and therefore, within reasonable bounds, the location of the moment reference is not particularly critical. The pitching-moment data have, therefore, been transferred to other moment-reference points, and the results are presented in figure 8(b). The results show that trim was obtained at the highest angle of attack by a forward shift of the moment reference a distance of 4.9 percent of the body length. Approximately the same trim conditions could have been achieved by moving the line confluence rearward on the body. The data presented in figure 8(b) for the moment-reference points at 47.1 and 42.9 percent of the body length show trim points at each end of the angle-of-attack range. A capability of shifting the center of gravity 4.2 percent of the body length would, therefore, allow the wing-body configuration to be trimmed throughout the usable lift-coefficient range.

Effects of longitudinal spread of rigging.- Inasmuch as the concept of the use of a high-fineness-ratio lifting body, such as that of the present investigation, may allow some freedom in selection of longitudinal spread of the rigging, the rest of the wind-tunnel investigation was directed toward variations in attachment geometry at the payload. A very large number of possible combinations of lines and attachment points at the payload could be achieved with a parawing having 23 suspension lines. The intent of the present rigging study was to survey briefly some of the most obvious possibilities in order to provide some background information for possible future application which could be studied in more detail when configuration requirements were more firmly determined.

The use of longitudinal spread in the rigging appeared attractive as a means for increasing the performance over that of a configuration having a point confluence, inasmuch as most of the longitudinal components of tension in the keel lines tend to compress the wing keel with a point-confluence rigging. A special rigging mount was used in order to obtain a much greater longitudinal spread of the lines than could be obtained on the body of configuration A. In initial tests made with the special mount, however, it was found that extreme forward location of the front lines would not allow the wing to inflate properly. The front-line attachment of configurations C, D, and E appeared to be at the most forward position that was practical for the wing used in this investigation.

Tests were made of the body alone and of the rigging-spread mount alone, and it was found that the aerodynamics of these components were insignificant in comparison with the wing aerodynamics. The assumption was made, therefore, that effects of attachment-point location could be shown by a comparison of data obtained for configurations A and C. The data for these configurations presented in figure 10 show that moving the front keel line forward caused an appreciable decrease in the wing angle of attack at a given sting angle. The lift coefficient was decreased from 0.9 to 0.8 and, as might be expected, the lift-drag ratios were increased. The highest lift-drag ratio of this investigation, about 2.7, was obtained for configuration C at the lowest sting angle of attack. There was little difference in pitching moment between configurations A and C at the lowest test angles of attack; however, at higher angles configuration C did not exhibit the abrupt loss of stability shown for configuration A (fig. 10). The slight improvement in stability for configuration C may have resulted from the restraint of the forward line, which would prevent the wing from rotating rearward as the sting angle increased.

Longitudinal aerodynamic characteristics of configuration B are presented in figure 11 for one value of dynamic pressure. Inasmuch as the three rear lines of this configuration had less than half as much elongation for a given load as those of configurations A and C, the results for configuration B are not directly comparable on the basis of attachment-point location. The results for configuration B are presented in figure 11 in order to show the variation of aerodynamic characteristics with angle of attack.

A comparison of configurations B, D, and E is made in connection with effects of dynamic pressure.

Appreciable effects of dynamic pressure on longitudinal aerodynamic characteristics were indicated for configuration A in tests conducted over an angle-of-attack range (fig. 8). Additional results were obtained to define the aerodynamic characteristics over a range of dynamic pressure at an angle of attack near that for maximum lift-drag ratio. The effects of longitudinal spread of the rigging of the three front lines are given in figure 12 by comparing data for configurations A and C over the range of test dynamic pressure. Effects of longitudinal rigging spread of the three front lines and six front lines are presented in figure 13 by comparing data for configurations B, D, and E. The results indicated that configurations with the rigging attachments spread longitudinally (configurations C, D, and E) had relatively small variations in aerodynamic characteristics with dynamic pressure. The data for configuration B also showed less variation with dynamic pressure than the data for configuration A, which had similar attachment points but more elasticity of the rear lines. The pitching-moment data for configurations D and E (fig. 13) show the positive increment that would be expected to accompany the transfer of three additional lines from the point confluence to the forward attachment point.

Free-Flight Tests

Free-flight tests were made on the wing from the wind-tunnel investigation and an aluminum body having the same dimensions as the wind-tunnel model. Objectives of the flight tests were to define the rigging for which stable gliding flight could be obtained and to define the magnitude of pitch-control travel (change in length of three rear lines) required to trim the model throughout its usable lift-coefficient range. Another objective was the determination of rigging requirements for maintaining the proper directional alinement of the body with respect to the wing in free flight. It should be noted that the line lengths labeled "basic flight" in figure 6 and table I were not obtained from the present wind-tunnel investigation but were obtained from a point-confluence rigging on another model which was tested both in the wind tunnel and in free flight with this rigging.

Point-confluence rigging.- Initial tests were made with the point-confluence rigging shown in figure 7(a) with the basic-flight line lengths given in figure 6 and table I. In these initial flights the model flew with a large pitch oscillation and unloading of the trailing edge was evident in the high angle-of-attack portion of the oscillation. These flight characteristics indicated that the wing was trimmed to fly at too high an angle of attack, and subsequent flights were made with the three rear lines lengthened. The model flew in steady forward flight when the three rear lines were lengthened about 1.0 percent of the keel length. Increasing the length of the three rear lines approximately

3.1 and 4.2 percent of the keel length in comparison with the basic-flight lengths also provided steady forward flight. When the lengthening of the three rear lines was increased to about 5.2 percent of the keel length the wing flew with the nose collapsed, which indicated that the lower limit of desirable wing angle of attack had been reached or exceeded. Therefore, the change in length of the three rear lines required to trim the model through its usable lift coefficient range was about 5 percent of the keel length.

Flights of the model with the point-confluence rigging showed unsatisfactory directional alinement of the body with respect to the wing. In several of the flights the body rotated about a vertical axis through the confluence point during most of the flight.

Longitudinal spread of rigging.- The poor directional alinement of the body obtained with the point-confluence rigging prompted a revised rigging-attachment configuration at the body as shown in figure 7(b). With the revised attachment configurations, steady trimmed flights were obtained and the wing and body were alined during all of these flights. No rotation tendency was evident in any of the flights with the rigging spread. It appears, therefore, that some longitudinal spread of the rigging would be required on any payload for which the touchdown orientation was important. As an alternate to longitudinal spread of the attachments, proper directional orientation of the payload might be achieved by fixed or controllable fins or jet-reaction controls. This possible alternate approach could be more useful where cross-wind landing capability is required.

CONCLUDING REMARKS

Low-speed wind-tunnel and flight tests were made to determine the static longitudinal aerodynamic characteristics and flight-rigging requirements for an all-flexible parawing proposed as a possible landing device for a lifting-body spacecraft.

The maximum lift-drag ratio measured in the wind-tunnel tests of the parawing and lifting-body combination was approximately 2.5 and the maximum lift coefficient obtained was about 0.96 for the highest test dynamic pressure. Decreasing the test dynamic pressure caused earlier collapse of the nose, which limited the minimum wing angle of attack and decreased the maximum lift-drag ratios of the parawing-body combination. Transfer of the three front suspension lines from the point confluence to an attachment point ahead of the confluence provided a maximum lift-drag ratio of 2.7 and a maximum lift coefficient of about 0.81.

Pitching-moment results indicated that the wing-body configuration was stable over the test angle-of-attack range for the assumed moment reference, except at the lowest test dynamic pressure where longitudinal instability occurred at high angles. These results also indicated that for longitudinal control by center-of-gravity shift, a capability of shifting the center of gravity relative to the wing by a distance of 4.2 percent of

the body length would allow the parawing-body configuration to be trimmed at any point in its usable lift-coefficient range.

Free-flight glide tests of the model indicated that the change in length of the three rear control lines required to trim the parawing-body combination over its usable lift coefficient range was about 5 percent of the keel length. In flight tests of the model with a point-confluence attachment of the lines, directional alinement characteristics of the body with respect to the wing were unsatisfactory. A modified rigging attachment that provided longitudinal spread of the attachment points at the body was found to give very good directional alinement of the body in flight.

Langley Research Center,
National Aeronautics and Space Administration,
Langley Station, Hampton, Va., January 17, 1967,
124-07-03-22-23.

REFERENCES

1. Bugg, Frank M.: Effects of Aspect Ratio and Canopy Shape on Low-Speed Aerodynamic Characteristics of 50.0° Swept Parawings. NASA TN D-2922, 1965.

2. Croom, Delwin R.; Naeseth, Rodger L.; and Sleeman, William C., Jr.: Effects of Canopy Shape on Low-Speed Aerodynamic Characteristics of a 55° Swept Parawing With Large-Diameter Leading Edges. NASA TN D-2551, 1964.

3. Naeseth, Rodger L.; and Gainer, Thomas G.: Low-Speed Investigation of the Effects of Wing Sweep on the Aerodynamic Characteristics of Parawings Having Equal-Length Leading Edges and Keel. NASA TN D-1957, 1963.

4. Phillips, W. Pelham: Low-Speed Longitudinal Aerodynamic Investigation of Parawings as Auxiliary Lifting Devices for a Supersonic Airplane Configuration. NASA TN D-2346, 1964.

5. Gillis, Clarence L.; Polhamus, Edward C.; and Gray, Joseph L., Jr.: Charts for Determining Jet-Boundary Corrections for Complete Models in 7- by 10-Foot Closed Rectangular Wind Tunnels. NACA WR L-123, 1945. (Formerly NACA ARR L5G31.)

6. Brown, W. S.: Wind Tunnel Corrections on Ground Effect. R & M. No. 1865, British A.R.C., 1939.

7. Herriot, John G.: Blockage Corrections for Three-Dimensional-Flow Closed-Throat Wind Tunnels, With Consideration of the Effect of Compressibility. NACA Rept. 995, 1950. (Supersedes NACA RM A7B28.)

TABLE I.- LINE LENGTHS

[Dimensions are in inches (centimeters)]

Line number[a]	Configuration A			Configuration B			Configuration C			Configuration D			Configuration E			Basic flight		
	Left	Keel	Right	Left	Keel	Right	Left	Keel	Right	Left	Keel	Right	Left	Keel	Right	Left	Keel	Right
1	103.5 (262.9)	100.6 (255.5)	103.2 (262.1)	102.5 (260.4)	101.5 (257.8)	102.0 (259.1)	107.2 (272.3)	107.0 (271.8)	106.5 (270.5)	107.2 (272.3)	107.0 (271.8)	106.5 (270.5)	107.2 (272.3)	107.0 (271.8)	106.5 (270.5)	105.2 (267.2)	104.6 (265.7)	105.2 (267.2)
2	98.3 (249.7)	101.0 (256.5)	98.4 (249.9)	97.2 (246.9)	100.4 (255.0)	96.8 (245.9)	98.3 (249.7)	101.0 (256.5)	98.4 (249.9)	98.3 (249.7)	101.0 (256.5)	98.4 (249.9)	103.4 (262.6)	106.8 (271.3)	102.2 (259.6)	99.9 (253.7)	103.7 (263.4)	99.9 (253.7)
3	94.5 (240.0)	101.0 (256.5)	94.4 (239.8)	93.8 (238.3)	101.0 (256.5)	93.0 (236.2)	94.5 (240.0)	101.0 (256.5)	94.4 (239.8)	94.5 (240.0)	101.0 (256.5)	94.4 (239.8)	94.5 (240.0)	101.0 (256.5)	94.4 (239.8)	96.2 (244.3)	103.0 (261.6)	96.2 (244.3)
4	90.2 (229.1)	100.4 (255.0)	89.8 (228.1)	90.2 (229.1)	99.8 (253.5)	90.0 (228.6)	90.2 (229.1)	100.4 (255.0)	89.8 (228.1)	90.2 (229.1)	100.4 (255.0)	89.8 (228.1)	90.2 (229.1)	100.4 (255.0)	89.8 (228.1)	91.7 (232.9)	102.6 (260.6)	91.7 (232.9)
5	85.9 (218.2)	98.8 (251.0)	85.8 (217.9)	85.8 (217.9)	98.8 (251.0)	85.5 (217.2)	85.9 (218.2)	98.8 (251.0)	85.8 (217.9)	85.9 (218.2)	98.8 (251.0)	85.8 (217.9)	85.9 (218.2)	98.8 (251.0)	85.8 (217.9)	87.7 (222.8)	101.1 (256.8)	87.7 (222.8)
6	69.1 (175.5)	97.6 (247.9)	69.4 (176.3)	68.2 (173.2)	97.8 (248.4)	68.5 (174.0)	68.2 (173.2)	97.6 (247.9)	68.1 (173.0)	68.0 (172.7)	97.6 (247.9)	68.5 (174.0)	67.0 (170.2)	97.6 (247.9)	67.5 (171.4)	79.4 (201.7)	99.7 (253.2)	79.4 (201.7)
7	------	96.8 (245.9)	------	------	96.8 (245.9)	------	------	96.8 (245.9)	------	------	96.8 (245.9)	------	------	96.8 (245.9)	------	------	98.4 (249.9)	------
8	------	95.2 (241.8)	------	------	95.2 (241.8)	------	------	95.2 (241.8)	------	------	95.2 (241.8)	------	------	95.2 (241.8)	------	------	97.0 (246.4)	------
9	------	92.8 (235.7)	------	------	92.9 (236.0)	------	------	92.8 (235.7)	------	------	92.8 (235.7)	------	------	92.8 (235.7)	------	------	95.0 (241.3)	------
10	------	88.8 (225.6)	------	------	89.5 (227.3)	------	------	88.8 (225.6)	------	------	88.8 (225.6)	------	------	88.8 (225.6)	------	------	92.2 (234.2)	------
11	------	74.9 (190.2)	------	------	77.0 (195.6)	------	------	77.8 (197.6)	------	------	79.0 (200.7)	------	------	76.0 (193.0)	------	------	84.8 (215.4)	------

[a]Lines numbered from front to rear of wing flat pattern.

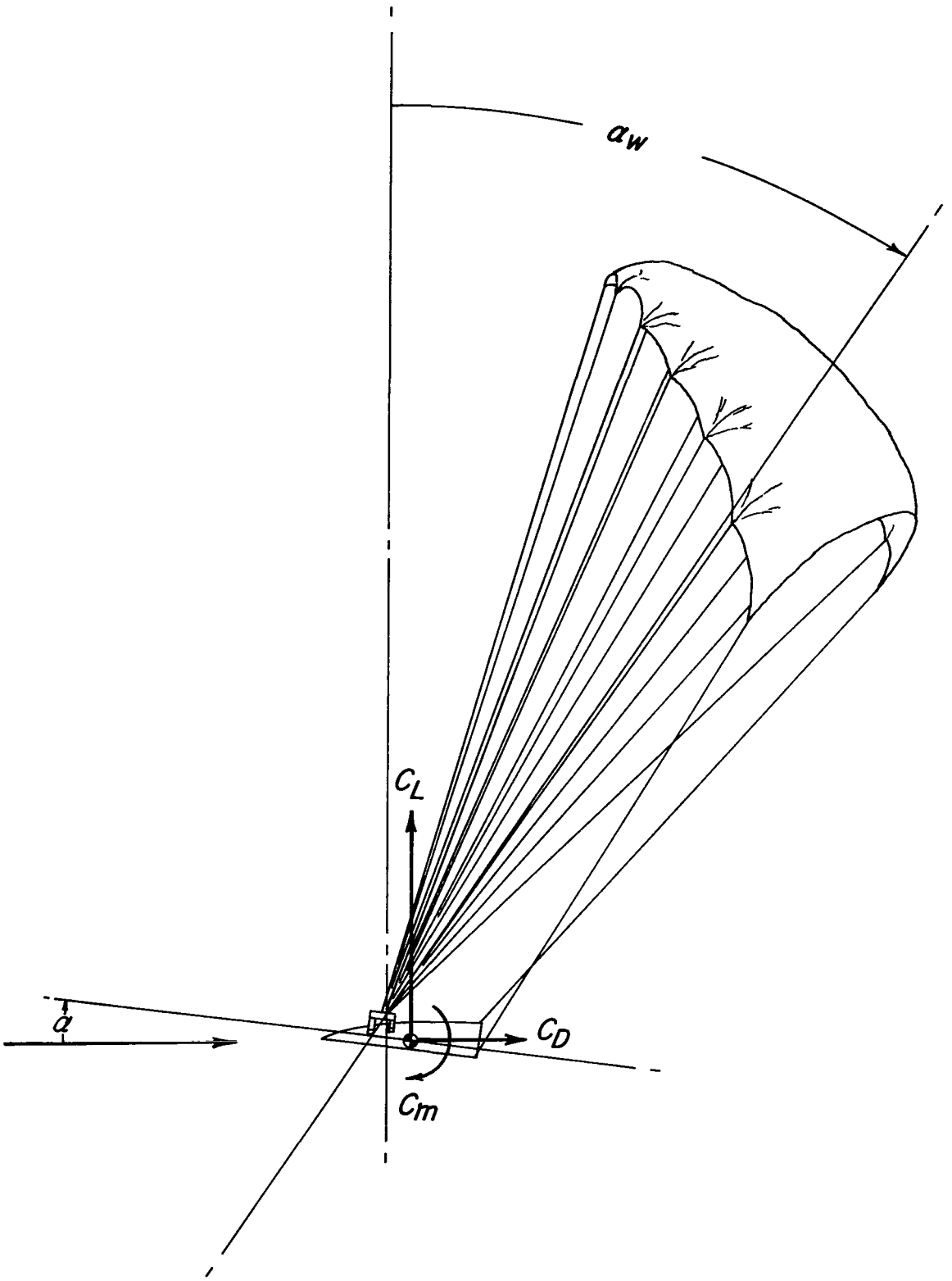

Figure 1.- System of axes used in presentation of the data. Positive directions are shown by arrows.

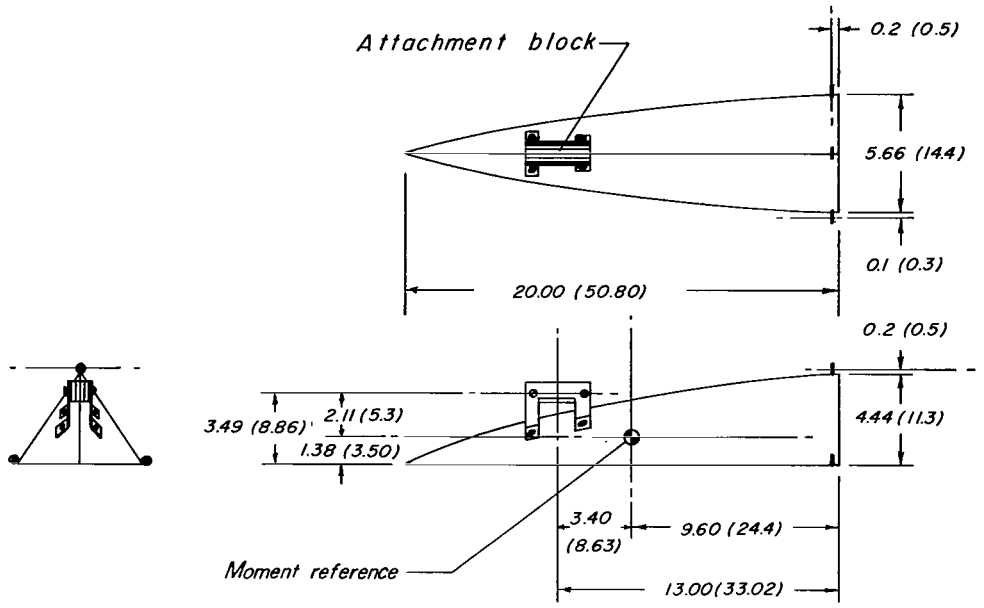

(a) Lifting body.

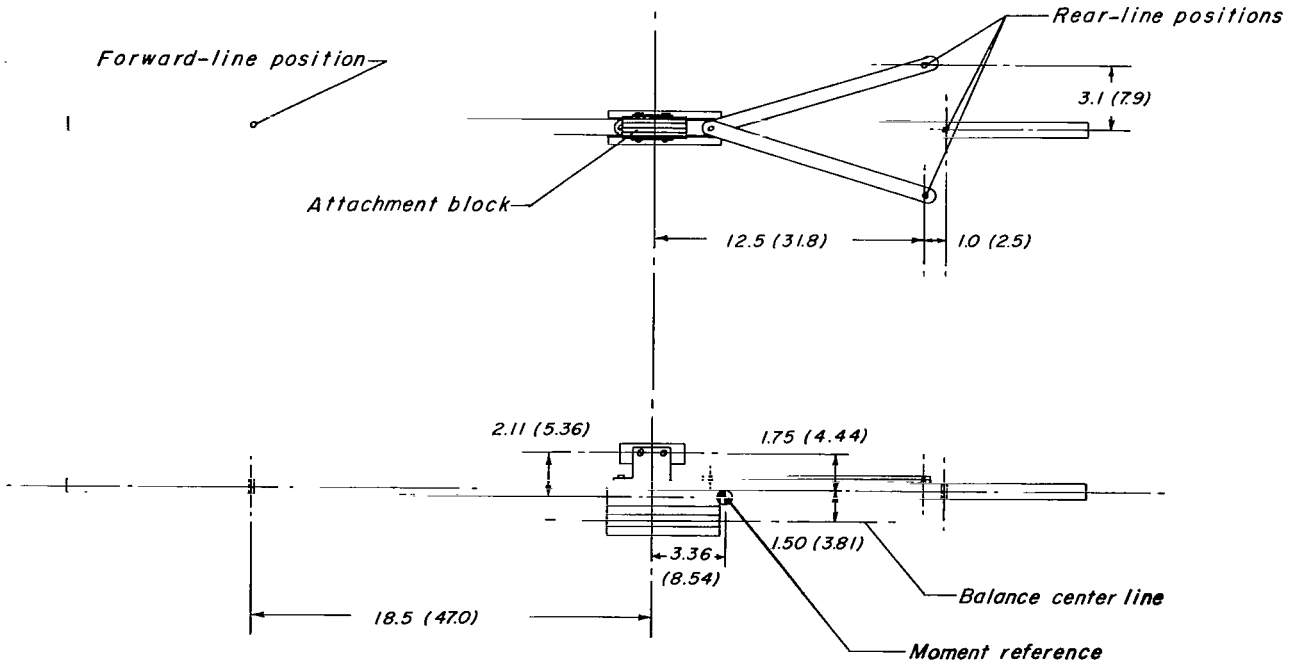

(b) Longitudinal rigging-spread mount.

Figure 2.- Geometric characteristics of mounting fixtures used in the tests.

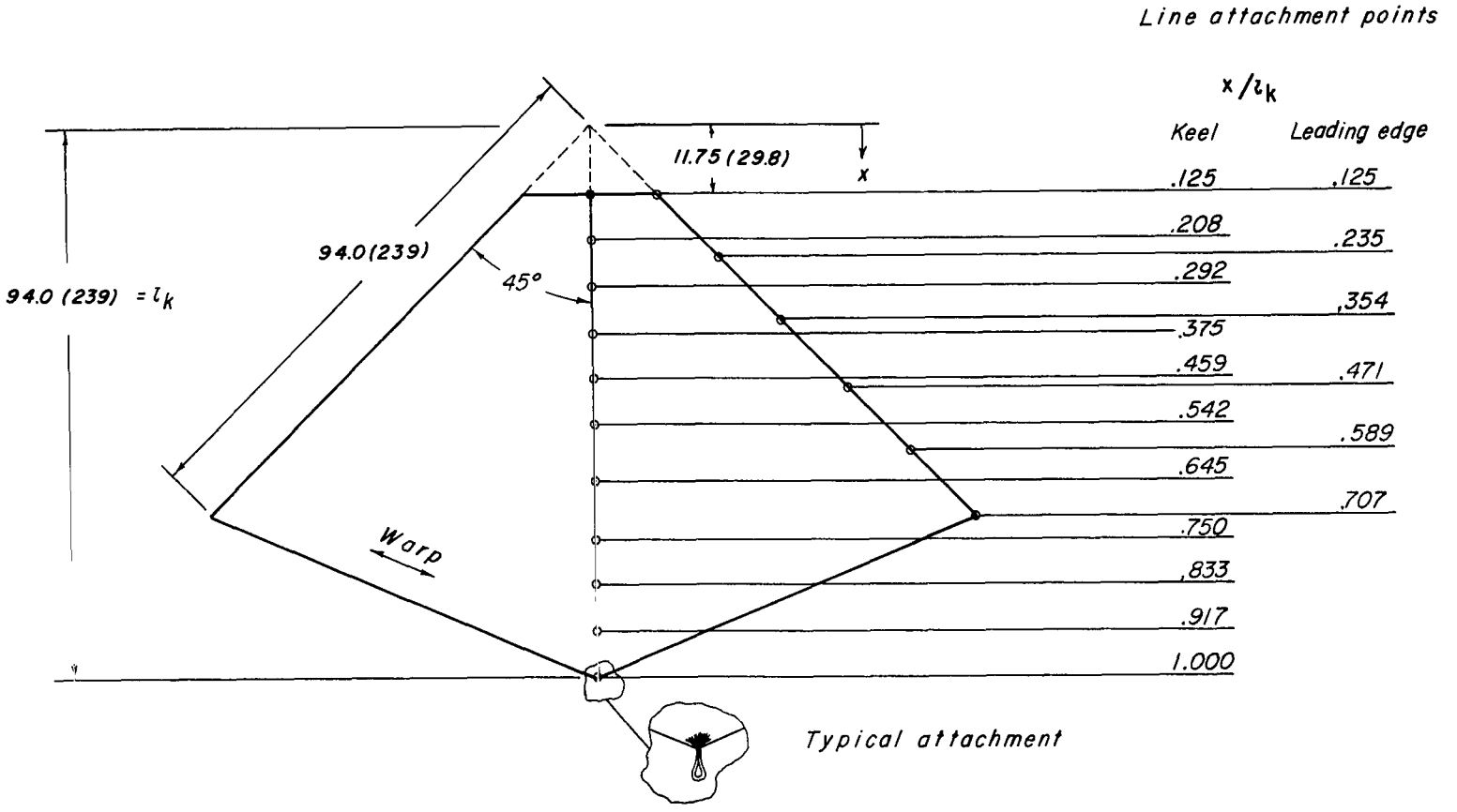

Figure 3.- Geometric characteristics of canopy flat pattern and location of line attachments on the all-flexible parawing model.

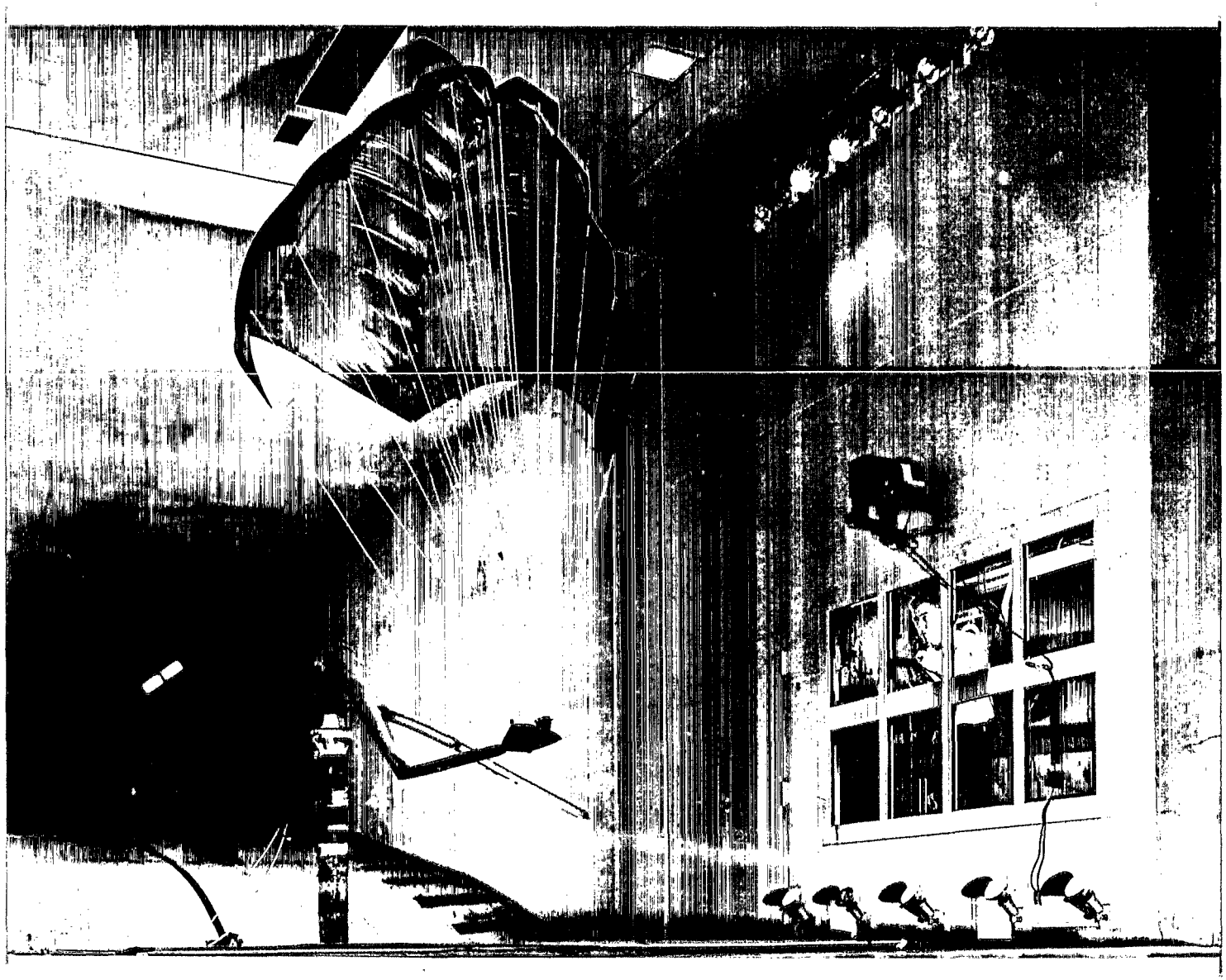

Figure 4.- Photograph of the all-flexible parawing configuration A in the 17-ft (5-m) test section of the Langley 300-MPH 7- by 10-foot tunnel. L-65-6478

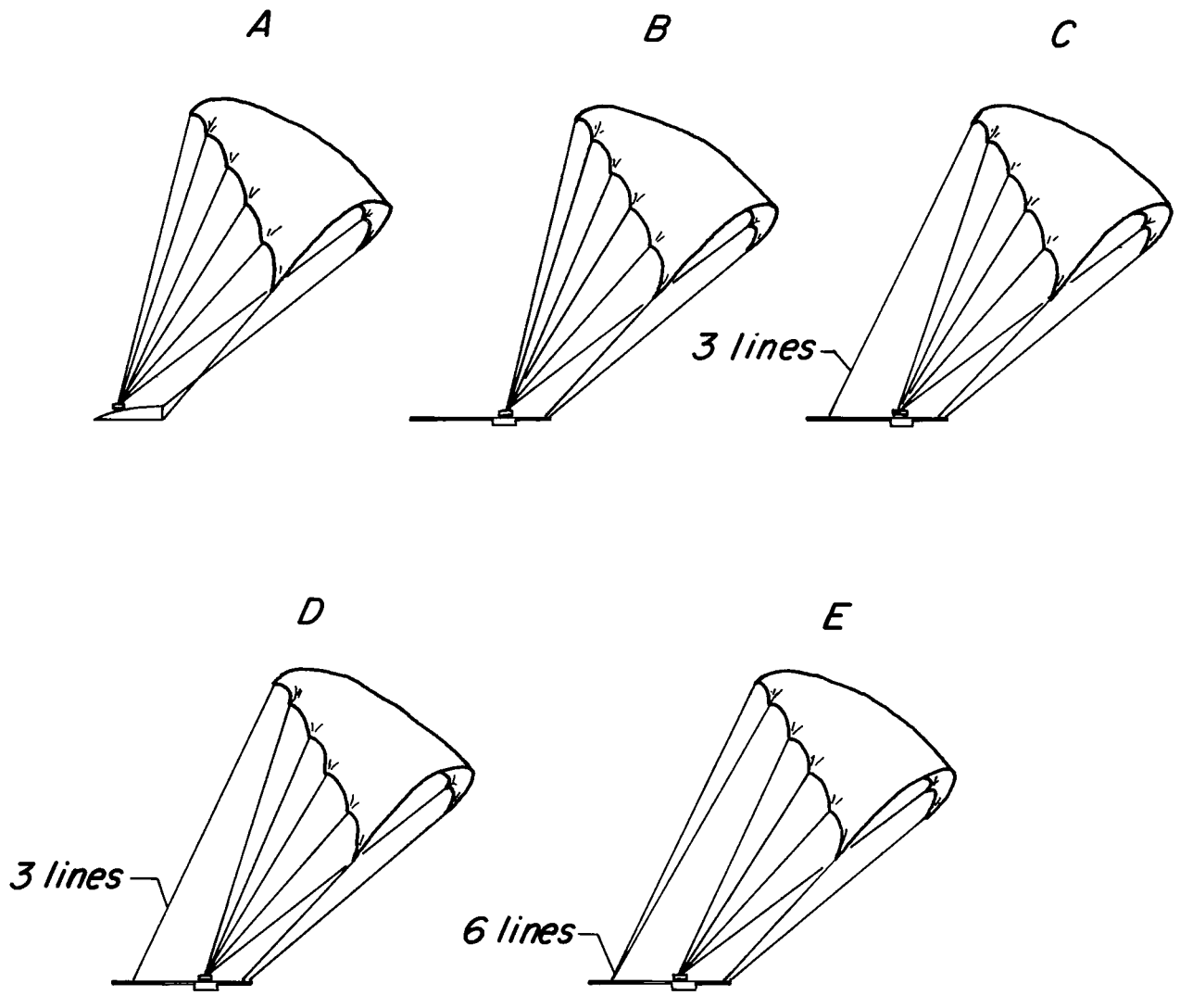

Configuration	Strength of three rear lines
A, C	100 lb (445 N)
B, D, E	550 lb (2440 N)

Figure 5.- Configurations tested in wind tunnel.

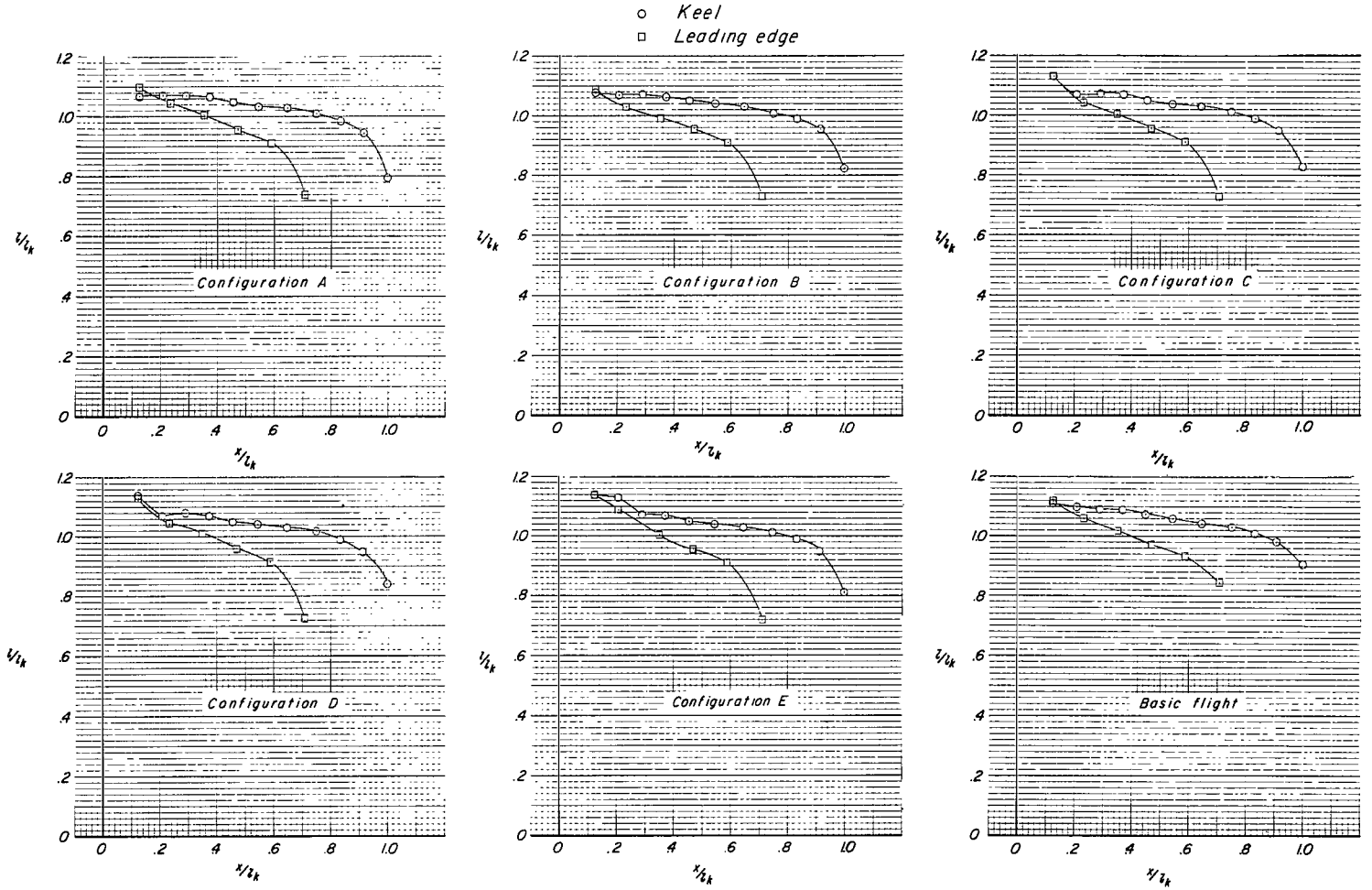

Figure 6.- Line lengths used in wind-tunnel and flight tests of the all-flexible parawing.

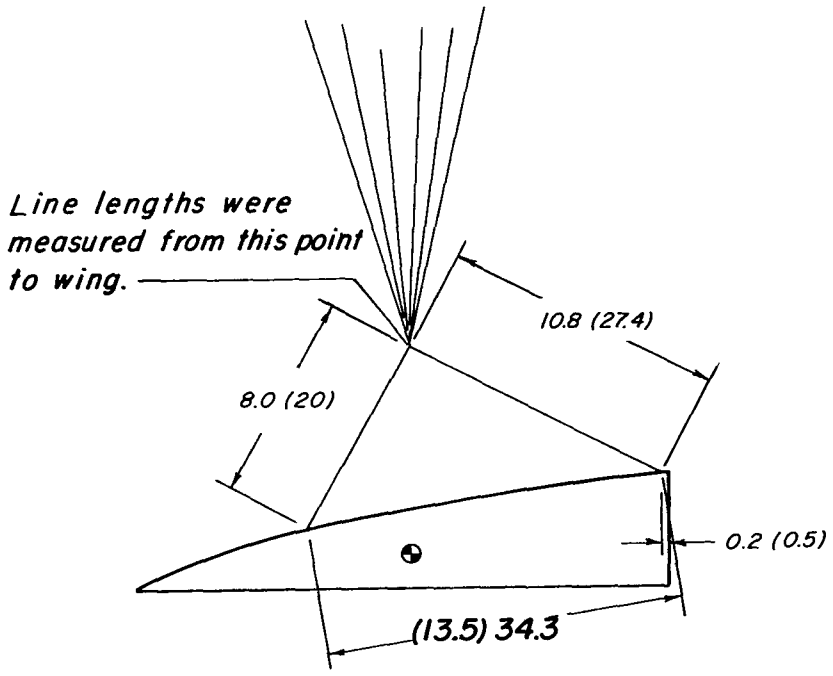

(a) Point-confluence rigging.

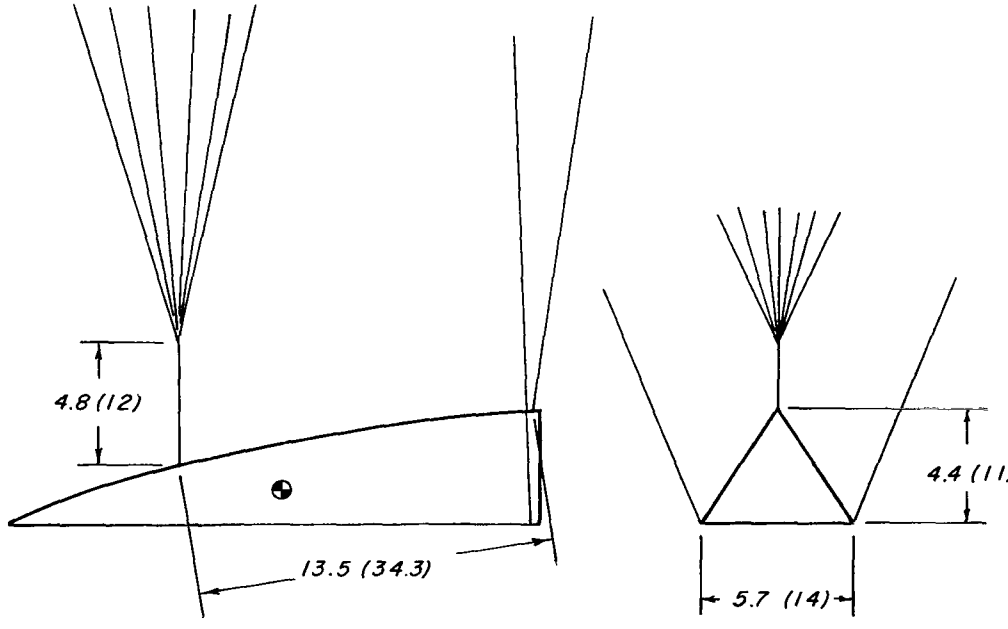

(b) Longitudinal spread of rigging.

Figure 7.- Systems of line attachment used in free-flight tests.

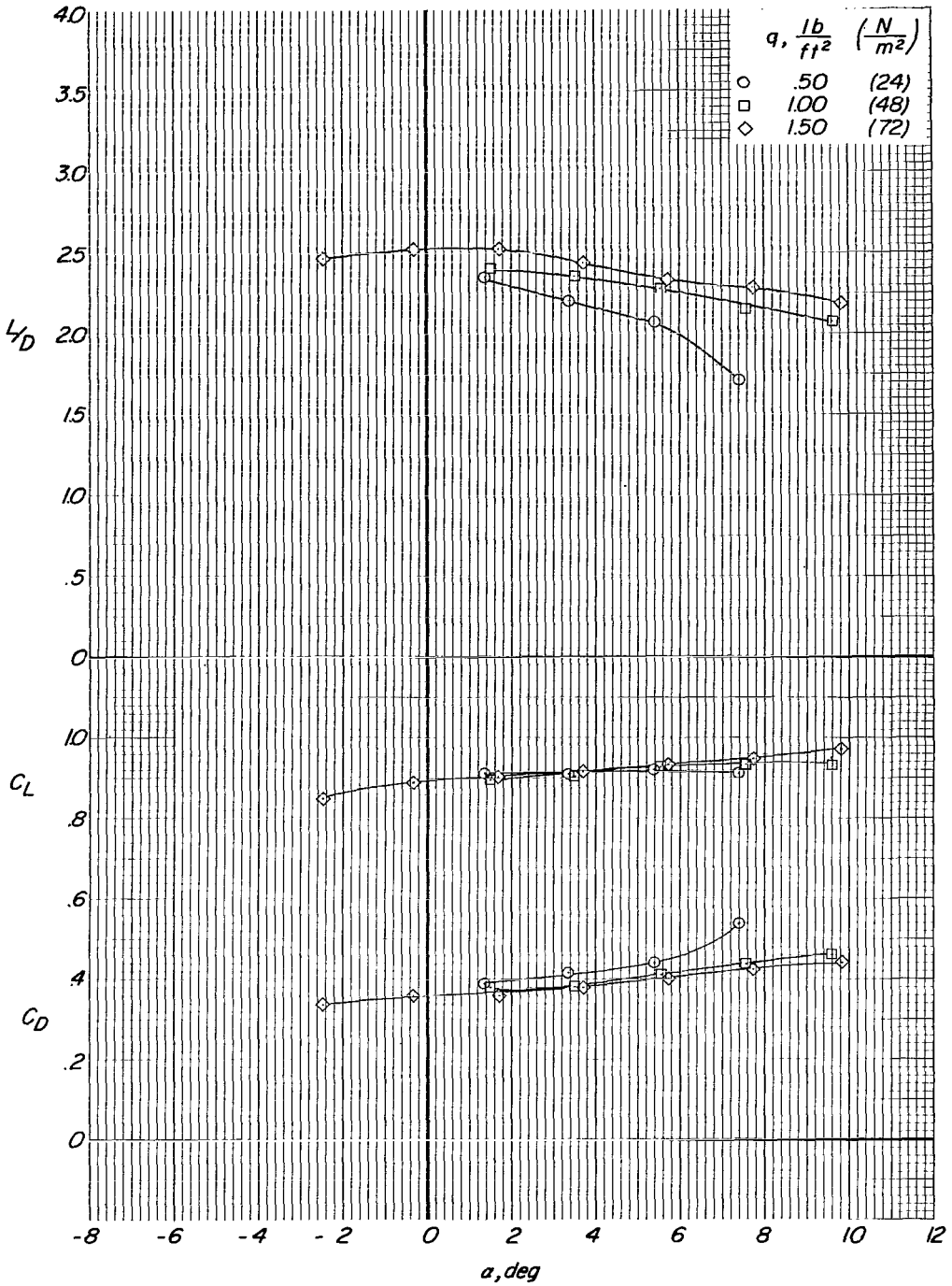

(a) Basic moment reference.

Figure 8.- Variation of longitudinal aerodynamic characteristics with angle of attack for configuration A.

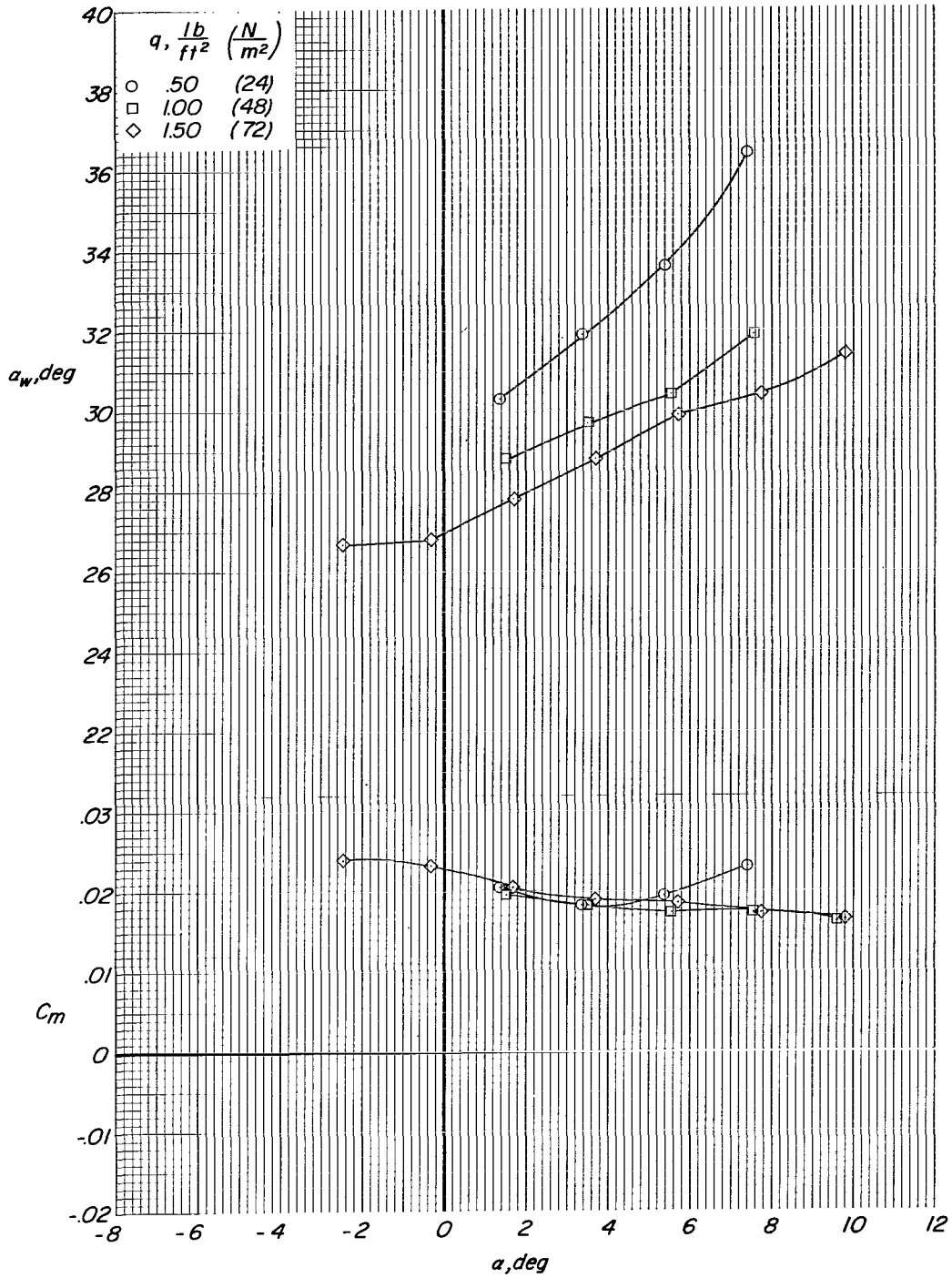

(a) Concluded.

Figure 8.- Continued.

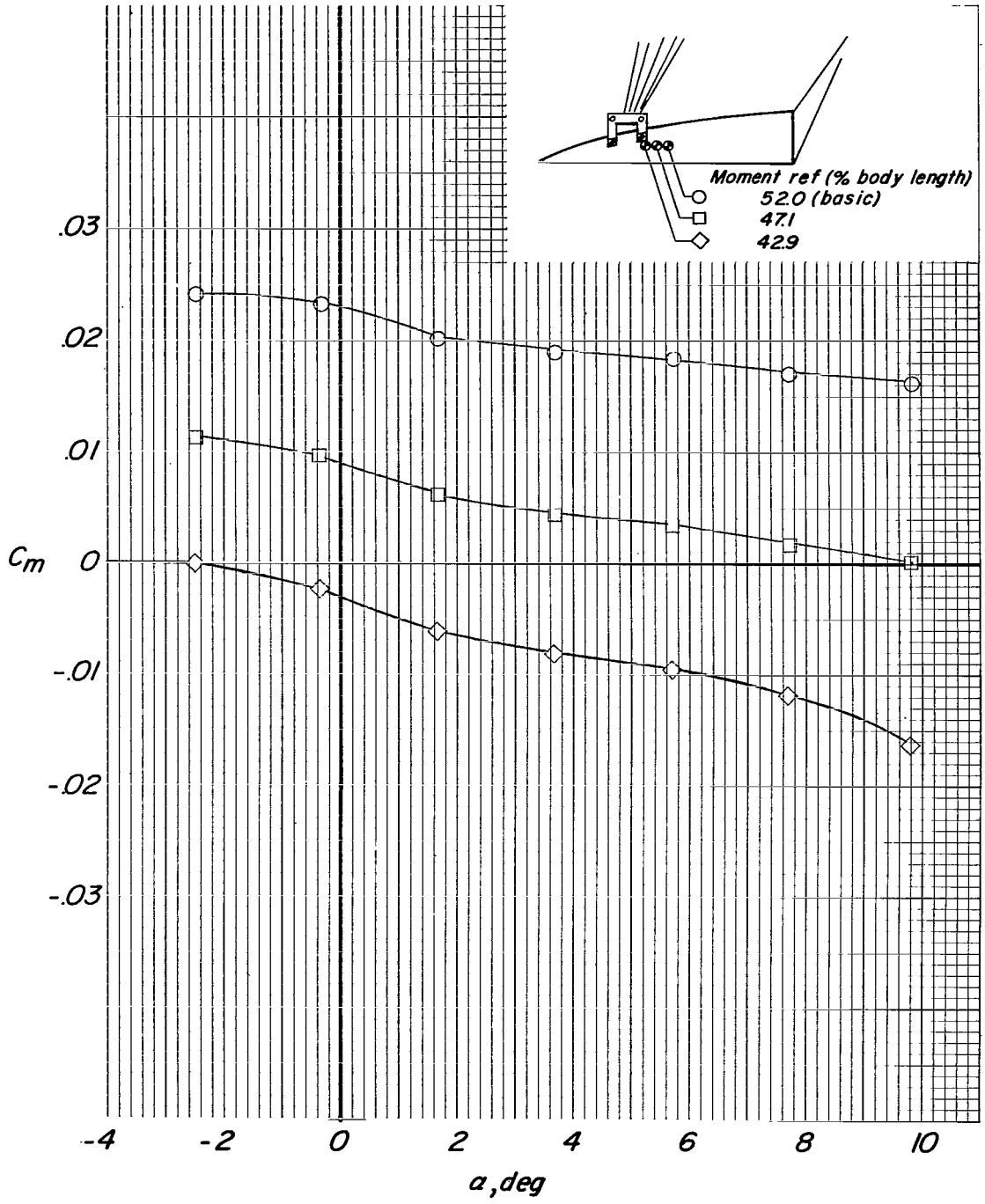

(b) Effect of longitudinal shift of moment reference at $q = 1.5$ lb/ft^2 (72 N/m^2).

Figure 8.- Concluded.

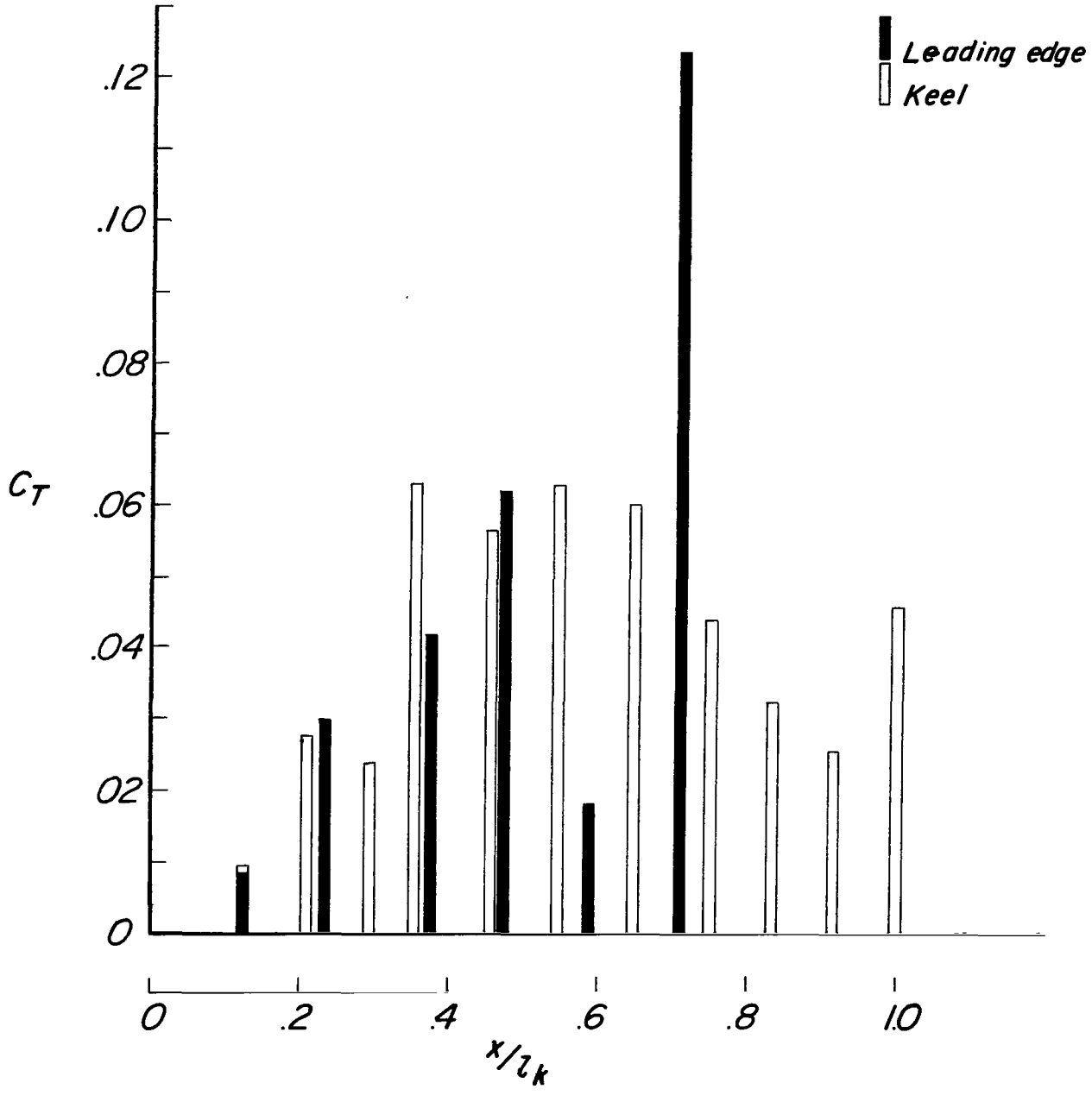

Figure 9.- Line-tension coefficients for configuration A at q = 1.0 lb/sq ft (47.9 N/m^2).

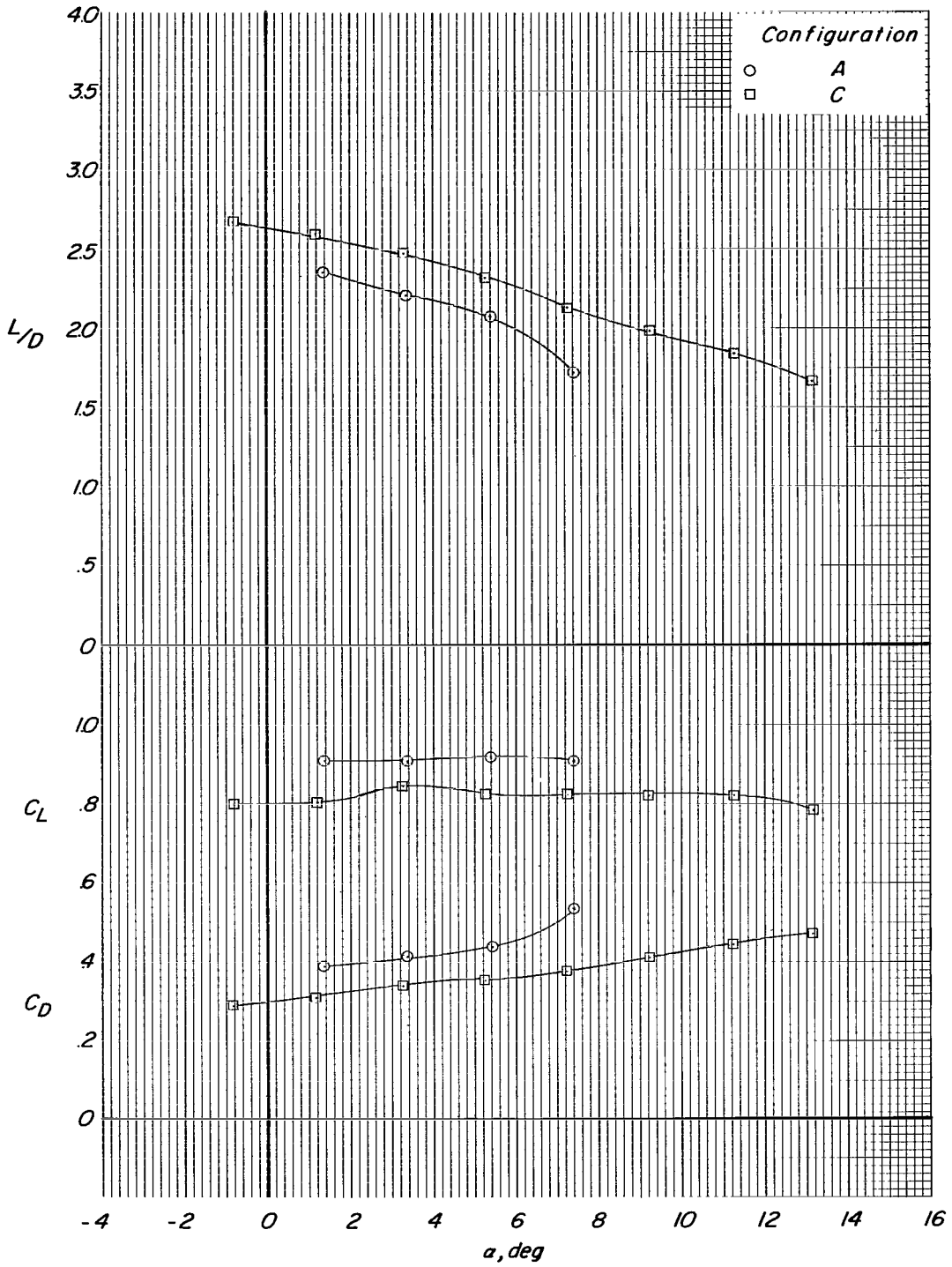

Figure 10.- Variation of longitudinal aerodynamic characteristics with angle of attack for configurations having different longitudinal rigging spread. q = 0.50 lb/ft^2 (24 N/m2).

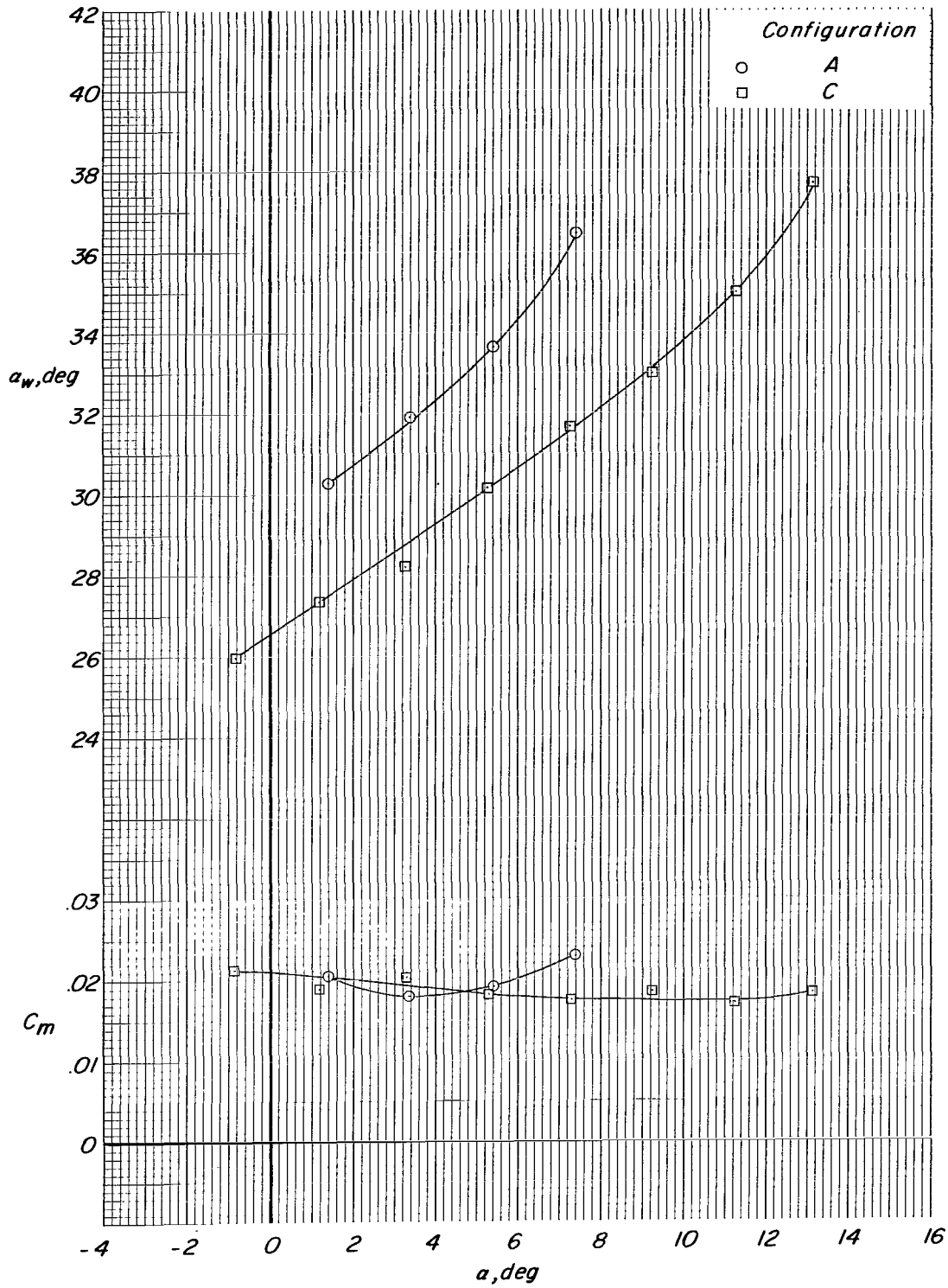

Figure 10.- Concluded.

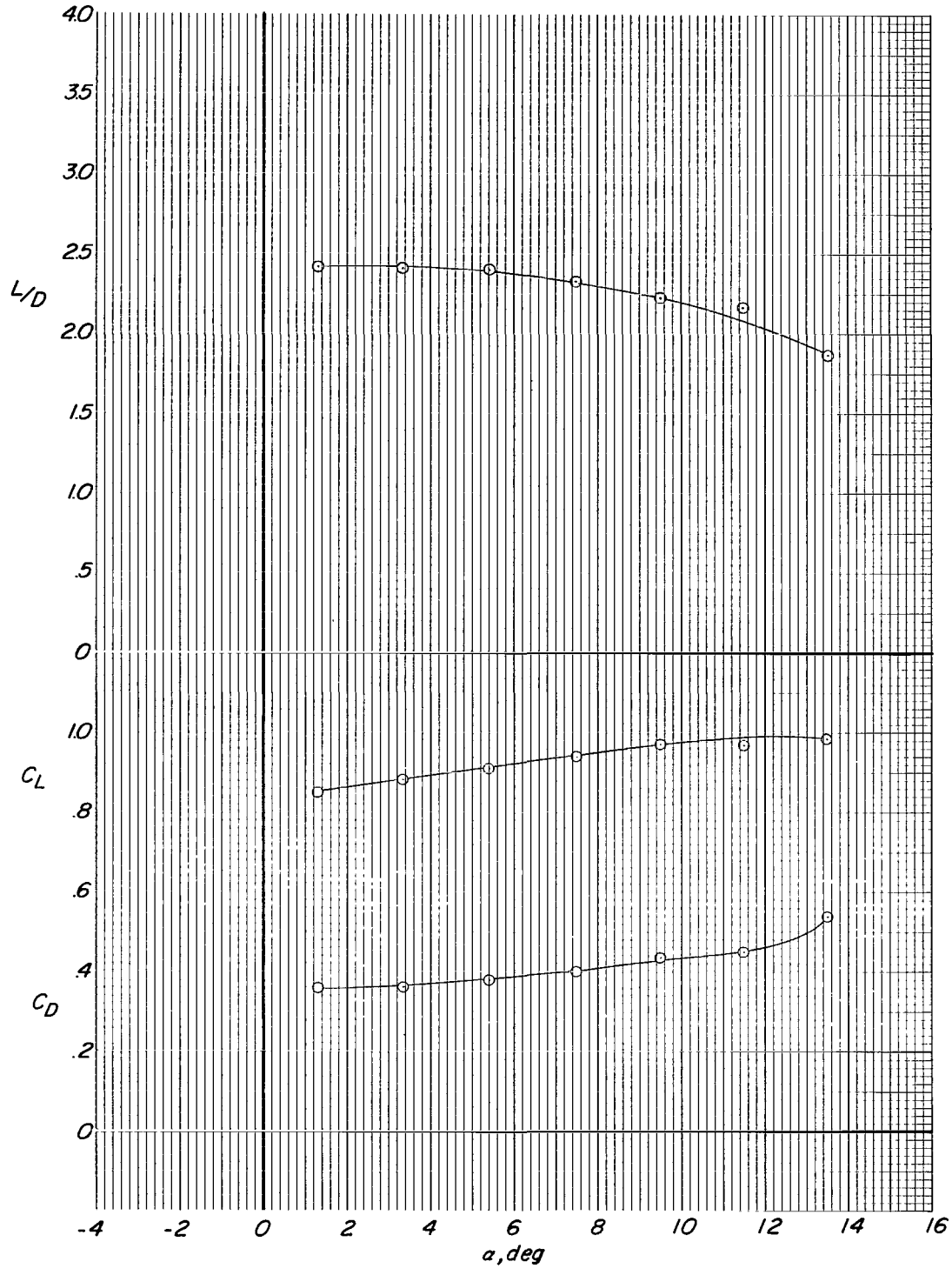

Figure 11.- Variation of longitudinal aerodynamic characteristics with angle of attack for configuration B. q = 0.75 lb/ft^2 (36 N/m2).

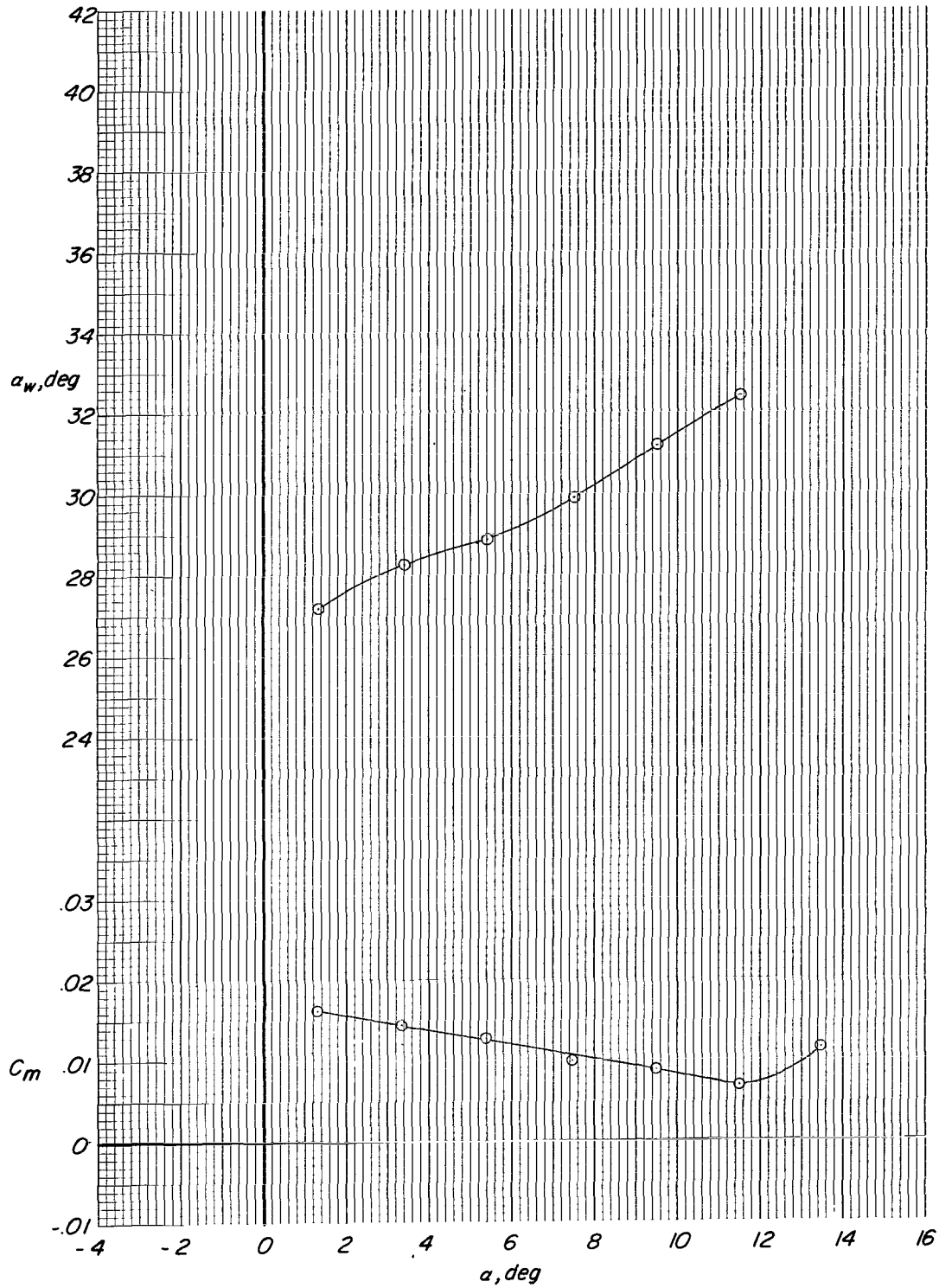

Figure 11.- Concluded.

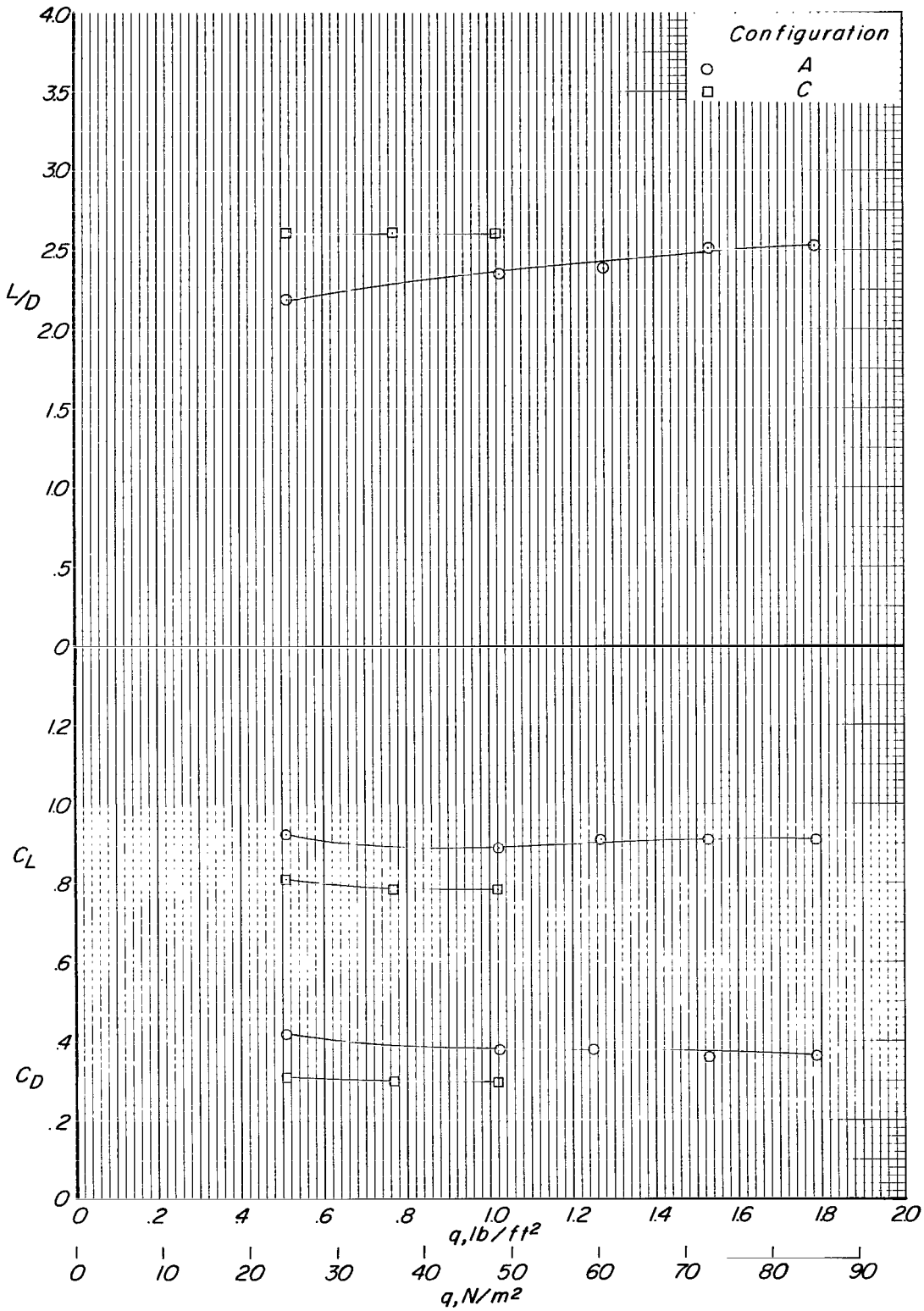

Figure 12.- Variation of longitudinal aerodynamic characteristics with test dynamic pressure for configurations A and C.

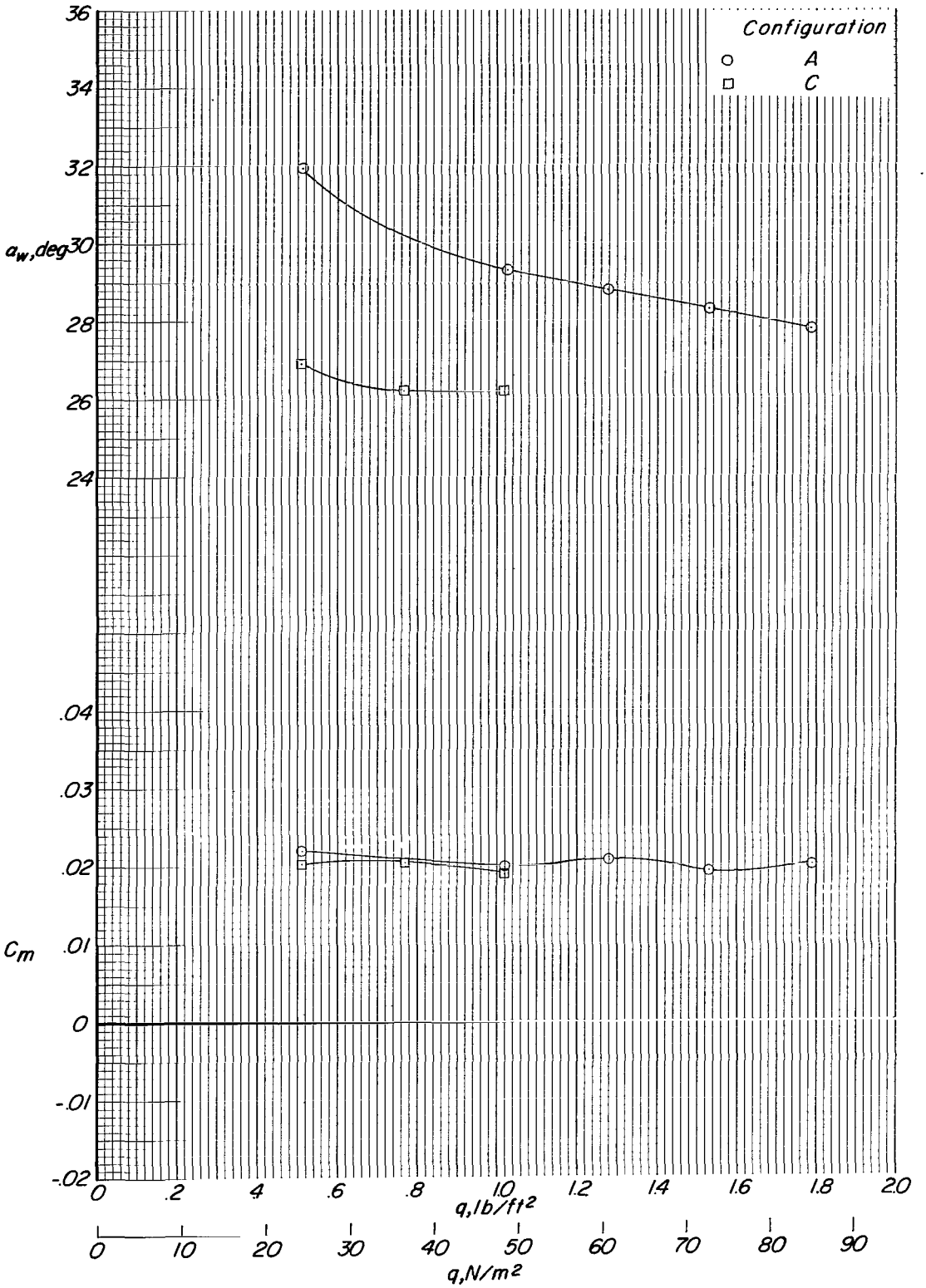

Figure 12.- Concluded.

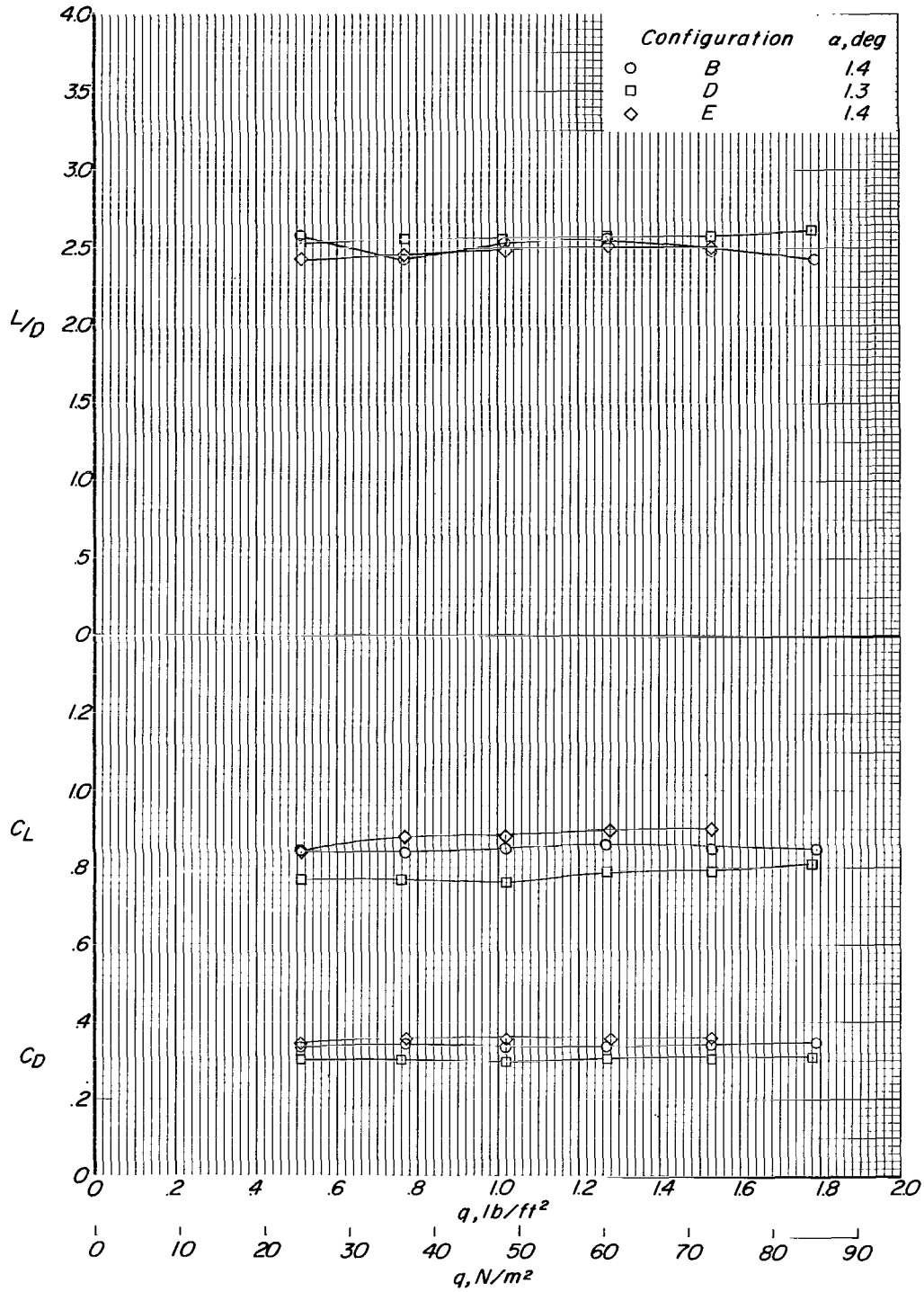

Figure 13.- Variation of longitudinal aerodynamic characteristics with test dynamic pressure for configurations B, D, and E.

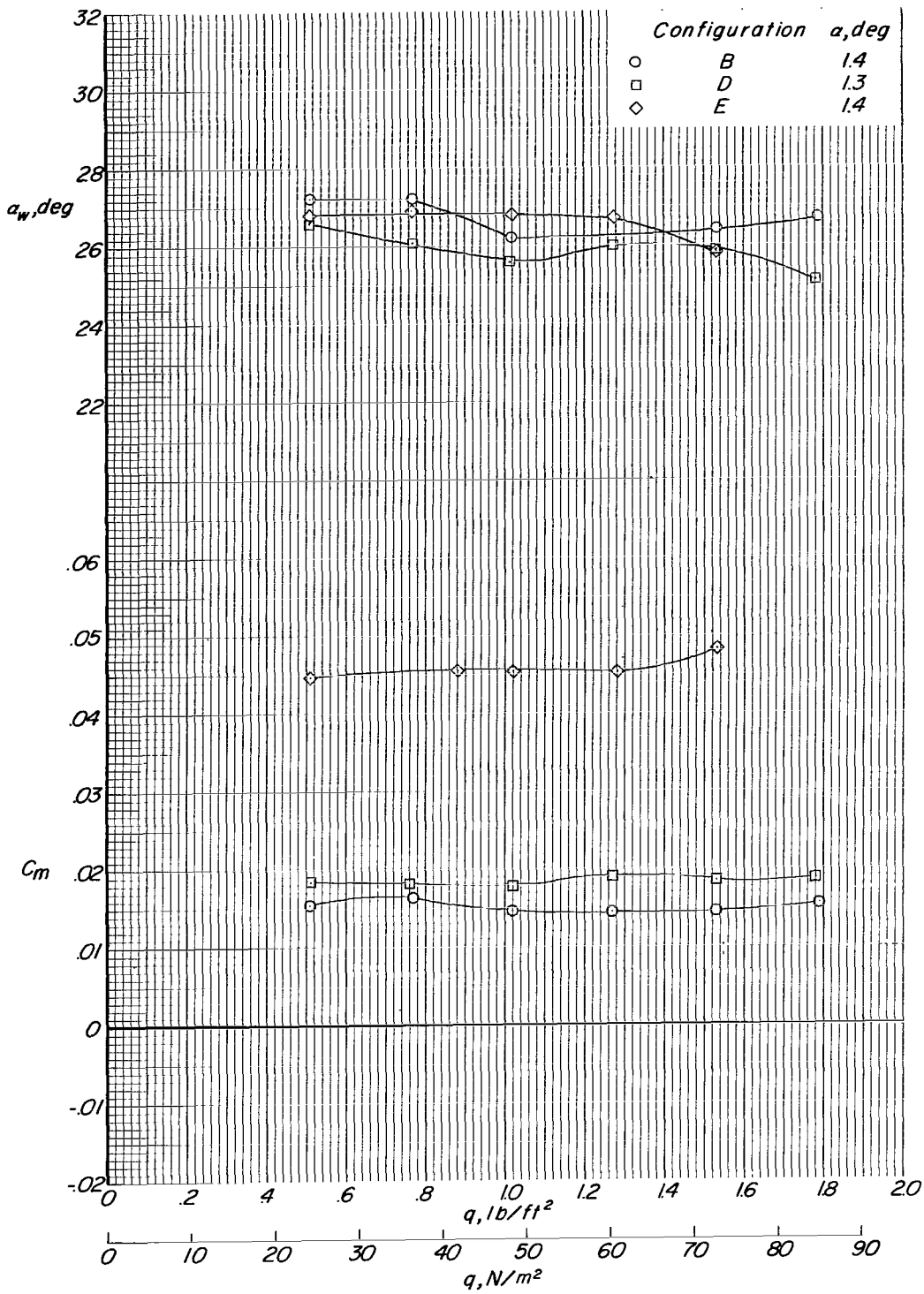

Figure 13.- Concluded.

NASA-Langley, 1967 —— 2 L-5228

"The aeronautical and space activities of the United States shall be conducted so as to contribute . . . to the expansion of human knowledge of phenomena in the atmosphere and space. The Administration shall provide for the widest practicable and appropriate dissemination of information concerning its activities and the results thereof."

—NATIONAL AERONAUTICS AND SPACE ACT OF 1958

NASA SCIENTIFIC AND TECHNICAL PUBLICATIONS

TECHNICAL REPORTS: Scientific and technical information considered important, complete, and a lasting contribution to existing knowledge.

TECHNICAL NOTES: Information less broad in scope but nevertheless of importance as a contribution to existing knowledge.

TECHNICAL MEMORANDUMS: Information receiving limited distribution because of preliminary data, security classification, or other reasons.

CONTRACTOR REPORTS: Scientific and technical information generated under a NASA contract or grant and considered an important contribution to existing knowledge.

TECHNICAL TRANSLATIONS: Information published in a foreign language considered to merit NASA distribution in English.

SPECIAL PUBLICATIONS: Information derived from or of value to NASA activities. Publications include conference proceedings, monographs, data compilations, handbooks, sourcebooks, and special bibliographies.

TECHNOLOGY UTILIZATION PUBLICATIONS: Information on technology used by NASA that may be of particular interest in commercial and other non-aerospace applications. Publications include Tech Briefs, Technology Utilization Reports and Notes, and Technology Surveys.

Details on the availability of these publications may be obtained from:

SCIENTIFIC AND TECHNICAL INFORMATION DIVISION

NATIONAL AERONAUTICS AND SPACE ADMINISTRATION

Washington, D.C. 20546